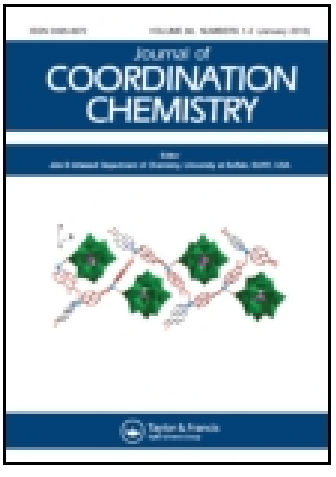

Journal of Coordination Chemistry
Publication details, including instructions for authors and subscription information:
http://www.tandfonline.com/loi/gcoo20

The synthesis, characterization, and electrochemistry of molecular cobaloxime/organocobaloxime: catalysts for cycloaddition of carbon dioxide and epoxides

Ahmet Kilic[a], Mahmut Ulusoy[a], Mustafa Durgun[a], Emine Aytar[a], Armagan Keles[a], Metin Dagdevren[b] & Ismail Yilmaz[b]
[a] Chemistry Department, Harran University, Sanliurfa, Turkey
[b] Chemistry Department, Istanbul Technical University, Istanbul, Turkey

Accepted author version posted online: 24 Jul 2014.Published online: 22 Aug 2014.

To cite this article: Ahmet Kilic, Mahmut Ulusoy, Mustafa Durgun, Emine Aytar, Armagan Keles, Metin Dagdevren & Ismail Yilmaz (2014) The synthesis, characterization, and electrochemistry of molecular cobaloxime/organocobaloxime: catalysts for cycloaddition of carbon dioxide and epoxides, Journal of Coordination Chemistry, 67:16, 2661-2679, DOI: 10.1080/00958972.2014.948431

To link to this article: http://dx.doi.org/10.1080/00958972.2014.948431

Journal of Coordination Chemistry, 2014
Vol. 67, No. 16, 2661–2679, http://dx.doi.org/10.1080/00958972.2014.948431

The synthesis, characterization, and electrochemistry of molecular cobaloxime/organocobaloxime: catalysts for cycloaddition of carbon dioxide and epoxides

AHMET KILIC*†, MAHMUT ULUSOY†, MUSTAFA DURGUN†, EMINE AYTAR†, ARMAGAN KELES†, METIN DAGDEVREN‡ and ISMAIL YILMAZ‡

†Chemistry Department, Harran University, Sanliurfa, Turkey
‡Chemistry Department, Istanbul Technical University, Istanbul, Turkey

(*Received 17 February 2014; accepted 13 June 2014*)

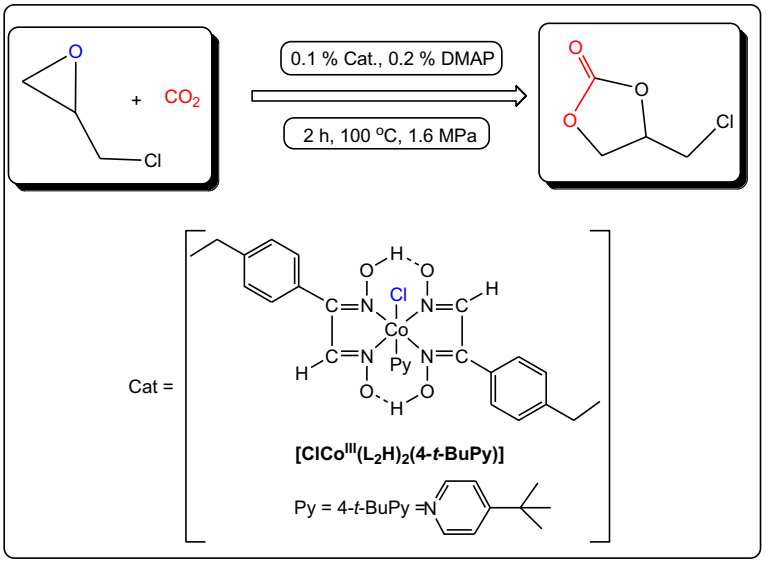

In this paper, the new cobaloxime (**1**), organocobaloxime (**2**) and multinuclear cobaloximes (**3**–**10**) were synthesized and characterized. These compounds were used as homogeneous catalysts for cyclic carbonate synthesis from carbon dioxide (CO_2) and epoxides.

The new cobaloxime (**1**), organocobaloxime (**2**), and their intramolecular hydrogen (O–H···O) bridges replaced by Cu(II)-containing multinuclear cobaloximes (**3**–**10**) were synthesized and characterized by elemental analysis, ^{1}H and ^{13}C NMR spectra, FT-IR spectra, UV–vis spectra, LC-MS spectra, molar conductivity measurements, melting point measurements, and magnetic susceptibility measurements. Their electrochemical properties were investigated using cyclic voltammetric techniques in DMSO solution. The cobaloxime or organocobaloxime (**1**, **2**) were used as precursors,

*Corresponding author. Email: kilica63@harran.edu.tr

replacing intramolecular O–H···O bridges, forming multinuclear complexes (**3**–**10**). Then, these compounds were used as homogeneous catalysts for cyclic carbonate synthesis from carbon dioxide (CO_2) and epoxides. In the catalytic experiments, dimethyl amino pyridine (DMAP) was used as co-catalyst, since DMAP was a more active base with higher yield compared to other Lewis bases. It is not necessary to use solvent according to catalytic test results, important in green chemistry.

Keywords: Cobaloxime; Organocobaloxime; Electrochemistry; Spectroscopy; Carbon dioxide

1. Introduction

Cobaloximes or organocobaloximes have the general formula $RCo(L_2)B$, where R is an organic group σ-bonded to cobalt, B is an axial base *trans* to the organic group, and L is a monoanionic dioxime ligand. The ligands glyoxime (gH), dimethylglyoxime (dmgH), 1,2-cyclohexanedione dioxime (chgH), diphenylglyoxime (dpgH), and other symmetric and unsymmetric dioximes are given as examples [1]. Cobaloximes and organocobaloximes with one or both of the intramolecular (O–H···O) bridges replaced by organoboryl groups are well known, but the intramolecular (O–H···O) bridges replaced by Cu(II) or other metal ions are not well known. Cobaloximes or organocobaloximes are known for H_2 production, easy to synthesize, oxygen-tolerant, amenable for coupling to natural and artificial photosynthetic systems, and rely only on earth-abundant materials [2, 3]. The pseudomacrocyclic cobaloxime compounds were originally developed and investigated as vitamin-B_{12} analogs [4] and have been extensively studied as a model system for vitamin B_{12} [5]. However, we have recently reported a different application area that molecular oxime complexes (such as $[Ni(dioxime)_2]$) are efficient and cheap homogeneous catalysts for cyclic carbonate synthesis from carbon dioxide (CO_2) and different epoxides [6]. In this study, we decided to synthesize new cobaloxime, organocobaloxime, and multinuclear complexes where the intramolecular hydrogen (O–H···O) bridges in the complex structure are replaced by Cu(II) ions. These target molecules have been used as catalysts for the coupling reactions of carbon dioxide (CO_2) with epoxides. While there are many literature reports on symmetric or unsymmetric dioxime ligands containing Co(III), they have not been used as catalysts for chemical fixation of carbon dioxide.

Carbon dioxide (CO_2) is considered to be the major cause of climate change because of its greenhouse properties and continuous accumulation in the atmosphere [7]. Scientific and industrial initiatives toward the chemical conversion of CO_2 have thus increased substantially [7–9]. For chemical conversion of carbon dioxide, many different binary/bifunctional catalyst systems have been reported by combining a Lewis acid and a nucleophile which is required for ring opening of the epoxide [10]. Chemical conversion of carbon dioxide is attractive in carbon chemistry because carbon dioxide as a renewable C_1 building block is an abundant, inexpensive, and nontoxic carbon source [11–14]. A promising methodology for chemical fixation of CO_2 is the cycloaddition of CO_2 to epoxides to form cyclic organic carbonates. Cyclic carbonates, such as ethylene carbonate (EC) and propylene carbonate (PC), are valuable organic synthetic intermediates, monomers, aprotic polar solvents, and pharmaceutical or fine chemical intermediates, and are applied broadly [14–16].

Herein, we described the new cobaloxime (**1**), organocobaloxime (**2**), and their intramolecular hydrogen (O–H···O) bridges replaced by Cu(II) complexes giving **3**–**10** that were characterized by elemental analysis, ^1H and ^{13}C NMR spectra, FT-IR spectra, UV–vis

spectra, LC-MS spectra, molar conductivity measurements, melting point measurements, and magnetic susceptibility measurements. Moreover, their electrochemical properties were investigated using cyclic voltammetric (CV) techniques in DMSO solution. All the compounds were used as catalysts in the direct synthesis of cyclic carbonates from carbon dioxide and epoxides. The optimal catalytic conditions were investigated by changing the epoxides, solvents, temperature, pressure, and time, consecutively.

2. Experimental

2.1. *Materials and methods*

All reagents and solvents were of reagent grade and obtained from commercial suppliers. Elemental analyses were performed by using LECO CHNS model 932 elemental analyzer. ^{1}H and ^{13}C NMR spectra were recorded on the Bruker-Avance 300 MHz spectrometer and chemical shifts are expressed in ppm relative to DMSO-d_6 at 25 °C. Infrared spectra were recorded in KBr on a Perkin Elmer Spectrum RXI FT-IR spectrometer (4000–400 cm^{-1}). Magnetic susceptibilities were determined on a Sherwood Scientific Magnetic Susceptibility Balance (Model MK1) at room temperature (25 °C) using $Hg[Co(SCN)_4]$ as a calibrant; diamagnetic corrections were calculated from Pascal's constants [6, 17]. UV–vis spectra were obtained on a Perkin-Elmer model Lambda 25 spectrophotometer from 200 to 1100 nm, and in C_2H_5OH and CH_2Cl_2 as solvents. Melting points were measured in open capillary tubes with an Electrothermal 9100 melting point apparatus and are uncorrected. Molar conductivities (Λ_M) were recorded on an Inolab Terminal 740 WTW Series. Mass spectra results were recorded on an Agilent LC/MSD LC-MS/MS spectrometer. CV measurements were carried out with an instrument (Princeton Applied Research Model 2263 potentiostat controlled by an external PC, using the computer program, Power CV) utilizing a three-electrode configuration at 25 °C. A platinum wire served as the counter electrode. An Ag/AgCl electrode was employed as the reference electrode. The working electrode was a platinum plate with an area of 0.2 cm^2. The working electrode was polished with Al_2O_3 prior to each experiment. Throughout the experiment, oxygen-free argon was bubbled through the solution for 10 min. Electrochemical grade tetrabutylammoniumperchlorate (TBAP) (0.2 M dm^{-3}) was employed as the supporting electrode. The origin 7.5 graphing program was used to evaluate Power CV data, to draw voltammograms, and to analyze them. Catalytic tests were performed in a PARR 4560 50 mL stainless steel pressure reactor. Gas chromatography was performed on an Agilent 7820A GC system with hydrogen as the carrier gas. Unsymmetric dioxime (LH_2) [6] and 1,10-phenanthroline-5,6-dione (dione) [18] were prepared according to literature procedures.

2.2. *Synthesis of $[ClCo^{III}(LH)_2(4\text{-}t\text{-}BuPy)]$ (1)*

In a typical reaction, cobalt(II) chloride hexahydrate ($CoCl_2{\cdot}6H_2O$) (1.86 g, 7.8 mM) was added to a stirred solution of the unsymmetric dioxime ligand (LH_2) (3.0 g, 15.6 mM) in 96% ethanol (100 mL). The mixture was vigorously stirred for 25 min with occasional swirling, during which the solution turned green and the mixture was again heated for 2 h under reflux. Later, the mixture was allowed to cool to room temperature and 4-*tert*-butylpyridine (1.06 g, 7.8 mM) was added to the mixture. Then water (10 mL) was added and a very gentle stream of air was passed through the solution for about 3 h to get the desired

product. The crude product obtained was recrystallized from CH_2Cl_2/C_2H_5OH (1 : 2). The product was collected, washed well with water, and air-dried. Color: dark brown, yield (%): 86, m.p: 180 °C, Anal. Calcd for [$C_{29}H_{35}N_5O_4ClCo$] (F·W: 612.0 g/M): C, 56.91; H, 5.76; N, 11.44. Found: C, 56.93; H, 5.74; N, 11.42. Λ_M = 16 Ω^{-1} cm^2 M^{-1}, μ_{eff} = Dia, LC-MS (Scan ES^+): *m/z* (%) 612.3 (6) $[M]^+$, 576.2 (15), 257.0 (22), 215.2 (18), and 214.2 (100), FT-IR (KBr pellets, υ_{max}/cm^{-1}): 3047 and 3026 υ(Ar–CH), 2964–2871 υ(Aliph–CH), 1718 υ(O–H···O), 1618 υ(C=N), 1544–1508 υ(C=C), 1273 υ(N–O), 509 and 486 υ(Co–N). ^{1}H NMR (DMSO-d_6, TMS, 300 MHz, δ ppm): 18.80 and 18.55 (s, 2H, O–*H*···O), 11.87 (s, 2H, *H*C=N), 8.64–8.09 and 7.57–7.24 (m, 12H, Ar–C*H*), 2.63–2.52 (q, 4H, CH_3–CH_2), 1.16 (t, 15H, *J* = 8.1 Hz, CH_3–CH_2 and *t*-BuPy-CH_3), ^{13}C NMR (DMSO-d_6, TMS, 75 MHz, δ ppm): 151.26 and 149.94 (C=NOH), 147.68, 146.16, 145.02, 141.28, 132.07, 130.35, and 128.47 (Ar–CH), 35.31 (*t*-BuPy-*C*–CH_3), 30.53 (*t*-BuPy-C–CH_3), 28.65 (CH_3–CH_2), and 16.03 (CH_3–CH_2). UV–vis (λ_{max}, nm, * = shoulder peak): 235, 260, 335, and 414* (C_2H_5OH); 233, 251, 326, and 416* (CH_2Cl_2).

2.3. *Synthesis of [PhCH$_2$Co^{III}(LH)$_2$(4-t-BuPy)] (2)*

A solution of NaOH (0.50 g, 12.5 mM) in water (5 mL) was added to a suspension of [$ClCo^{III}(LH)_2$(4-*t*-BuPy)] (**1**) (1.50 g, 2.45 mM) in about 100 mL of absolute ethanol, the mixture was kept under a blanket of nitrogen (N_2) for 30 min and was cooled to 0 °C with stirring. The mixture turned blue after addition of NaOH solution. After 5 min, the color of solution immediately turned orange on addition of benzyl bromide (2.13 g, 12.42 mM), followed by a solution of sodium borohydride ($NaBH_4$) (0.90 g, 23.68 mM) in water (10 mL). The reaction mixture was stirred at −2 °C for 3 h, then the nitrogen blanket was removed and the mixture was exposed to air and 10 mL of acetone and 10 mL of water were added. The mixture was stirred for 20 min, then the volume of the reaction mixture was reduced to 10 mL by evaporation and poured into 30 mL water. The resulting brown precipitate was filtered, washed with hexane and diethyl ether, and air-dried. The product was recrystallized from CH_2Cl_2/C_2H_5OH (1 : 2) solution and finally dried *in vacuum*. Color: gold yellow, yield (%): 76, m.p: 176 °C, Anal. Calcd for [$C_{36}H_{42}N_5O_4Co$] (F·W: 667.7 g/M): C, 64.76; H, 6.34; N, 10.49. Found: C, 64.78; H, 6.32; N, 10.48%. Λ_M = 17 Ω^{-1} cm^2 M^{-1}, μ_{eff} = Dia, LC-MS (Scan ES^+): *m/z* (%) 667.4 (6) $[M]^+$, 320.2 (35), 226.2 (100), and 179.1 (20). FT-IR (KBr pellets, υ_{max}/cm^{-1}): υ(O–H···O), 3086 and 3030 υ(Ar–CH), 2964–2871 υ(Aliph–CH), 1724 υ(O–H···O), 1609 υ(C=N), 1550–1512 υ(C=C), 1272 υ(N–O), 508 and 500 υ(Co–N). ^{1}H NMR (DMSO-d_6, TMS, 300 MHz, δ ppm): 18.36 and 18.16 (s, 2H, O–*H*···O), 8. 90 (s, 2H, *H*C=N), 8.11 (s, 4H, Ar–C*H*), 7.62–7.21 (m, 13H, Ar–C*H*), 5.46 (s, 2H, Ph–CH_2), 2.52 (s, 4H, CH_3–CH_2), 1.19 (t, 9H, *J* = 9.2 Hz, *t*-BuPy-CH_3) and 1.05 (s, 6H, CH_3–CH_2), ^{13}C NMR (DMSO-d_6, TMS, 75 MHz, δ ppm): 152.45 and 148.96 (C=NOH), 148.03, 146.23, 145.08, 140.86, 137.01, 132.15, 130.28, 129.64, 128.46 and 128.39 (Ar–CH), 78.43 (CH_2–Ph), 36.29 (*t*-BuPy-*C*–CH_3), 29.91 (*t*-BuPy-C–CH_3), 28.99 (CH_3–CH_2), and 16.04 (CH_3–CH_2). UV–vis (λ_{max}, nm, * = shoulder peak): 266 and 381* (C_2H_5OH); 236, 265, and 381* (CH_2Cl_2).

2.4. *Synthesis of the [{Cu(N–N)}$_2$ClCo^{III}(L)$_2$(4-t-BuPy)](ClO$_4$)$_2$ complexes (3–6)*

In a two-neck, 100-mL round-bottom flask and equipped with a blanket of nitrogen (N_2) was placed 70 mL of 95% ethanol. [$ClCo^{III}(LH)_2$(4-*t*-BuPy)] (**1**) (0.50 g, 0.82 mM) and

Et_3 N (3 mL) were added slowly with stirring to this solution, consecutively. The solution was brought to reflux over 1 h. To this solution were successively added separate solutions of $Cu(ClO_4)_2{\cdot}6H_2O$ (0.62 g, 1.64 mM) in 95% ethanol (15 mL) and 2,2′-bipyridine (bpy) (0.26 g, 1.64 mM), 1,10-phenanthroline monohydrate (phen) (0.32 g, 1.64 mM), 1,10-phenanthroline-5,6-dione (dione) (0.34 g, 1.64 mM), and 4,4′-ditertbutyl-2,2′-bipyridine (dtbpy) (0.44 g, 1.64 mM) in 95% ethanol (10 mL) as bidentate ligands, followed by boiling under reflux for 6 h to synthesize three new multinuclear complexes having the general formulas $[\{Cu(N\text{-}N)\}_2ClCo^{III}(L)_2(4\text{-}t\text{-}BuPy)](ClO_4)_2$ (**3**–**6**). The dark brown color of the mononuclear $[ClCo^{III}(LH)_2(4\text{-}t\text{-}BuPy)]$ (**1**) changed to pale brown or green upon formation of the multinuclear $[\{Cu(N\text{–}N)\}_2ClCo^{III}(L)_2(4\text{-}t\text{-}BuPy)](ClO_4)_2$ (**3**–**6**) complexes. Then the mixtures were left for 48 h to precipitate. The solvent was evaporated slowly at room temperature and the products were recrystallized from CH_2Cl_2/EtOH (1 : 2) to give pale brown or green crystals that were filtered, then washed with water and Et_2O, and dried in air.

2.4.1. For $[\{Cu(bpy)\}_2ClCo^{III}(L)_2(4\text{-}t\text{-}BuPy)](ClO_4)_2$ (3). Color: green; yield (%): 73, m.p: 138 °C, Anal. Calcd for $[C_{49}H_{49}N_9O_{12}Cl_3Cu_2Co]$ (F·W: 1248.4 g/M): C, 47.14; H, 3.96; N, 10.10. Found: C, 47.13; H, 3.97; N, 10.13%. Λ_M = 154 Ω^{-1} cm^2 M^{-1}, μ_{eff} = 1.59 [B.M]. (for per Cu(II) ion), LC-MS (Scan ES^+): *m/z* (%) 1248.4 (10) $[M]^+$, 827.0 (17), 681.2 (100), 567.1 (95) and 400.9 (15). FT-IR (KBr pellets, υ_{max}/cm^{-1}): 3113–3032 υ(Ar–CH), 2964–2872 υ(Aliph–CH), 1604 υ(C=N *oxime*), 1573 υ(C=N *bpy*), 1508–1473 υ(C=C), 1251 υ(N–O), 1090 and 624 υ(ClO_4), 517 υ(Co–N), 473 υ(Cu–N), and 459 υ(Cu–O). UV–vis (λ_{max}, nm, * = shoulder peak): 252, 298, 313 and 631* (C_2H_5OH); 252, 304, 315* and 624* (CH_2Cl_2).

2.4.2. For $[\{Cu(phen)\}_2ClCo^{III}(L)_2(4\text{-}t\text{-}BuPy)](ClO_4)_2$ (4). Color: green; yield (%): 74, m.p: 229 °C, Anal. Calcd for $[C_{53}H_{49}N_9O_{12}Cl_3Cu_2Co]$ (F·W: 1296.4 g/M): C, 49.10; H, 3.81; N, 9.72. Found: C, 49.12; H, 3.80; N, 9.70%. Λ_M = 148 Ω^{-1} cm^2 M^{-1}, μ_{eff} = 1.58 [B.M]. (for per Cu(II) ion), LC-MS (Scan ES^+): *m/z* (%) 1296.5 (15) $[M]^+$, 1117.1 (35), 961.0 (100), 901.9 (50), 767.0 (55), and 403.1 (65), FT-IR (KBr pellets, υ_{max}/cm^{-1}): 3065 and 3026 υ(Ar–CH), 2963–2871 υ(Aliph–CH), 1603 υ(C=N *oxime*), 1585 υ(C=N *phen*), 1519–1458 υ(C=C), 1270 υ(N–O), 1090 and 623 υ(ClO_4), 506 υ(Co–N), 476 υ(Cu–N) and 454 υ(Cu–O). UV–vis (λ_{max}, nm, * = shoulder peak): 224, 271, 293* and 389* (C_2H_5OH); 233, 272, 297, 396 and 642* (CH_2Cl_2).

2.4.3. For $[\{Cu(dione)\}_2ClCo^{III}(L)_2(4\text{-}t\text{-}BuPy)](ClO_4)_2$ (5). Color: green; yield (%): 72, m.p: 206 °C, Anal. Calcd for $[C_{53}H_{45}N_9O_{16}Cl_3Cu_2Co]$ (F·W: 1356.4 g/M): C, 46.93; H, 3.34; N, 9.29. Found: C, 46.91; H, 3.35; N, 9.31%. Λ_M = 153 Ω^{-1} cm^2 M^{-1}, μ_{eff} = 1.61 [B.M]. (for per Cu(II) ion), LC-MS (Scan ES^+): *m/z* (%) 1357.2 (15) $[M+H]^+$, 764.6.0 (55), 681.3 (100), 470.3 (20) and 239.2 (30), FT-IR (KBr pellets, υ_{max}/cm^{-1}): 3080 υ(Ar–CH), 2969–2802 υ(Aliph–CH), 1722 υ(C=O), 1602 υ(C=N *oxime*), 1591 υ(C=N *dione*), 1512–1434 υ(C=C), 1272 υ(N–O), 1090 and 625 υ(ClO_4), 504 υ(Co–N), 463 υ(Cu–N) and 456 υ(Cu–O). UV–vis (λ_{max}, nm, * = shoulder peak): 233, 255, 282 and 347* (C_2H_5OH); 223, 262 and 316* (CH_2Cl_2).

2.4.4. For [{Cu(dtbpy)}$_2$ClCo^{III}(L)$_2$(4-t-BuPy)](ClO$_4$)$_2$ (6). Color: brown; yield (%): 70, m.p: 212 °C, Anal. Calcd for [$C_{65}H_{81}N_9O_{12}Cl_3Cu_2Co$] (F·W: 1472.7 g/M): C, 53.01; H, 5.54; N, 8.56. Found: C, 52.98; H, 5.52; N, 8.57%. Λ_M = 157 Ω^{-1} cm^2 M^{-1}, μ_{eff} = 1.62 [B.M]. (for per Cu(II) ion), LC-MS (Scan ES$^+$): *m/z* (%) 1472.3 (20) [M]$^+$, 769.3 (40), 681.2 (100), 605.1 (35) and 432.9 (40), FT-IR (KBr pellets, υ_{max}/cm^{-1}): 3062 and 3021 υ(Ar–CH), 2964–2872 υ(Aliph–CH), 1604 υ(C=N *oxime*), 1549 υ(C=N *dtbpy*), 1511–1464 υ(C=C), 1252 υ(N–O), 1090 and 623 υ(ClO_4), 506 υ(Co–N), 484 υ(Cu–N), and 456 υ(Cu–O). UV–vis (λ_{max}, nm, * = shoulder peak): 256, 296, 310 and 626* (C_2H_5OH); 234, 259, 297, 310 and 619* (CH_2Cl_2).

2.5. *Synthesis of the [{Cu(N–N)}$_2$PhCH$_2$Co^{III}(L)$_2$(4-t-BuPy)](ClO$_4$)$_2$ complexes (7–10)*

In a two-neck, 100-mL round-bottom flask and equipped with a blanket of nitrogen (N_2) was placed 60 mL of 95% ethanol. To this solution was added [$PhCH_2Co^{III}(LH)_2$(4-*t*-BuPy)] (**2**) (0.60 g, 0.90 mM) slowly with stirring, followed by Et_3 N (5 mL). The solution was brought to reflux for 2 h. To this mixture, a separate solution of $Cu(ClO_4)_2 \cdot 6H_2O$ (0.68 g, 1.80 mM) for all the three complexes [{Cu(N–N)}$_2$$PhCH_2Co^{III}(L)_2$(4-*t*-BuPy)] ($ClO_4$)$_2$ (**7**–**10**) in 95% ethanol (10 mL) and 2,2′-bipyridine (bpy) (0.29 g, 1.80 mM), 1,10-phenanthroline monohydrate (phen) (0.35 g, 1.80 mM)), 1,10-phenanthroline-5,6-dione (dione) (0.37 g, 1.80 mM), and 4,4′-ditertbutyl-2,2′-bipyridine (dtbpy) (0.48 g, 1.50 mM) in 95% ethanol (15 mL) was successively added separately, and then the mixture was refluxed for 8 h. The gold yellow color of mononuclear [$PhCH_2Co^{III}(LH)_2$(4-*t*-BuPy)] (**2**) changed to brown or green upon formation of the trinuclear [{Cu(N–N)}$_2$$PhCH_2Co^{III}(L)_2$(4-*t*-BuPy)] ($ClO_4$)$_2$ (**7**–**10**) complexes. Then the mixtures were left for 48 h to precipitate. The solvent was evaporated slowly at room temperature and the products were recrystallized from CH_2Cl_2/EtOH (1 : 2) to give brown or green crystals that were filtered, then washed with water and Et_2O, and dried in air.

2.5.1. For [{Cu(bpy)}$_2$PhCH$_2$Co^{III}(L)$_2$(4-t-BuPy)](ClO$_4$)$_2$ (7). Color: green; yield (%): 68, m.p: 184 °C, Anal. Calcd for [$C_{56}H_{56}N_9O_{12}Cl_2Cu_2Co$] (F·W: 1304.0 g/M): C, 51.58; H, 4.33; N, 9.67. Found: C, 51.56; H, 4.35; N, 9.68%. Λ_M = 158 Ω^{-1} cm^2 M^{-1}, μ_{eff} = 1.61 [B.M]. (for per Cu(II) ion), LC-MS (Scan ES$^+$): *m/z* (%) 1304.2 (12) [M]$^+$, 656.1 (25), 561.1 (85), 410.2 (20) and 320.2 (100). FT-IR (KBr pellets, υ_{max}/cm^{-1}): 3117–3030 υ(Ar–CH), 2964–2871 υ(Aliph–CH), 1606 υ(C=N *oxime*), 1574 υ(C=N *bpy*), 1555–1473 υ(C=C), 1249 υ(N–O), 1090 and 624 υ(ClO_4), 508 υ(Co–N), 479 υ(Cu–N), and 458 υ(Cu–O). UV–vis (λ_{max}, nm, * = shoulder peak): 250, 298. 313* and 381* (C_2H_5OH); 249, 301, 313 and 384* (CH_2Cl_2).

2.5.2. For [{Cu(phen)}$_2$PhCH$_2$Co^{III}(L)$_2$(4-t-BuPy)](ClO$_4$)$_2$ (8). Color: brown; yield (%): 70, m.p: 229 °C, Anal. Calcd for [$C_{60}H_{56}N_9O_{12}Cl_2Cu_2Co$] (F·W: 1352.1 g/M): C, 53.30; H, 4.18; N, 9.32. Found: C, 58.33; H, 4.16; N, 9.31%. Λ_M = 146 Ω^{-1} cm^2 M^{-1}, μ_{eff} = 1.62 [B.M]. (for per Cu(II) ion), LC-MS (Scan ES *m/z* (%) 1352.3 (30) [M]$^+$, 1138.4 (100), 982.8 (90), 316.9 (45) and 256.6 (48). FT-IR (KBr pellets, υ_{max}/cm^{-1}): 3062 and 3030 υ(Ar–CH), 2963–2865 υ(Aliph–CH), 1603 υ(C=N *oxime*), 1586 υ(C=N *phen*), 1520–1454 υ(C=C), 1271 υ(N–O), 1090 and 624 υ(ClO_4), 508 υ(Co–N), 487 υ(Cu–N), and 458 υ(Cu–O). UV–vis (λ_{max}, nm, * = shoulder peak): 224, 271 and 386* (C_2H_5OH); 233, 271, 301 and 386* (CH_2Cl_2).

2.5.3. For [{Cu(dione)}$_2$PhCH$_2$Co^{III}(L)$_2$(4-t-BuPy)](ClO$_4$)$_2$ (9). Color: brown; yield (%): 73, m.p: 246 °C, Anal. Calcd for [$C_{60}H_{52}N_9O_{16}Cl_2Cu_2Co$] (F·W: 1412 g/M): C, 51.04; H, 3.71; N, 8.93. Found: C, 51.05; H, 3.70; N, 8.94%. Λ_M = 156 Ω^{-1} cm^2 M^{-1}, μ_{eff} = 1.55 [B.M]. (for per Cu(II) ion), LC-MS (Scan ES$^+$): *m/z* (%) 1412.2 (35) [M]$^+$, 1383.3 (50), 1016.2 (53), 959.9 (100) and 927.0 (60), FT-IR (KBr pellets, υ_{max}/cm^{-1}): 3083 and 3030 υ(Ar–CH), 2964–2872 υ(Aliph–CH), 1722 and 1710 υ(C=O), 1606 υ(C=N *oxime*), 1575 υ(C=N *dione*), 1513–1428 υ(C=C), 1269 υ(N–O), 1090 and 624 υ(ClO$_4$), 500 υ(Co–N), 488 υ(Cu–N) and 467 υ(Cu–O). UV–vis (λ_{max}, nm, * = shoulder peak): 232, 264 and 383* (C_2H_5OH); 234, 263 and 389* (CH_2Cl_2).

2.5.4. For [{Cu(dtbpy)}$_2$PhCH$_2$Co^{III}(L)$_2$(4-t-BuPy)](ClO$_4$)$_2$ (10). Color: brown; yield (%): 68, m.p: 136 °C, Anal. Calcd for [$C_{72}H_{88}N_9O_{12}Cl_2Cu_2Co$] (F·W: 1528.5 g/M): C, 56.58; H, 5.80; N, 8.25. Found: C, 56.56; H, 5.79; N, 8.27%. Λ_M = 158 Ω^{-1} cm^2 M^{-1}, μ_{eff} = 1.64 [B.M]. (for per Cu(II) ion), LC-MS (Scan ES$^+$): *m/z* (%) 1529.4 (15) [M + H]$^+$, 785.3 (100), 679.2 (25), 362.2 (25) and 226.2 (100), FT-IR (KBr pellets, υ_{max}/cm^{-1}): 3061 and 3022 υ(Ar–CH), 2965–2872 υ(Aliph–CH), 1605 υ(C=N *oxime*), 1549 υ(C=N *dtbpy*), 1512–1462 υ(C=C), 1252 υ(N–O), 1090 and 624 υ(ClO$_4$), 508 υ(Co–N), 488 υ(Cu–N) and 458 υ(Cu–O). UV–vis (λ_{max}, nm, * = shoulder peak): 248, 263, 297, 311 and 367* (C_2H_5OH); 234, 262, 298 and 376* (CH_2Cl_2).

2.6. *General procedure of coupling reaction of epoxides and CO$_2$*

All coupling reactions were performed in a 50-mL stainless steel autoclave equipped with a mechanical stirrer. The autoclave reactor was successively charged with cobaloxime or organocobaloxime complexes (4.5×10^{-5} M), epoxide (4.5×10^{-2} M), and dimethyl amino pyridine (DMAP) (9×10^{-5} M). The reaction vessel was placed under a constant pressure of carbon dioxide for 2 min to allow the system to equilibrate and CO_2 was charged into the autoclave at the desired pressure, then was heated and stirred at the desired reaction temperature. The pressure was kept constant during the reaction. When the pressure of CO_2 fell to 1–3 atm, the reactor was cooled quickly to 5–10 °C in an ice bath after the desired reaction time. The pressure was released and the excess gasses were vented. The crude product in $CDCl_3$ was analyzed by ^{1}H NMR spectroscopy and FT-IR to determine if any polycarbonate, epoxides, DMAP, or other byproducts were present. The peak at 1795 cm^{-1} was attributed to the carbonyl group in cyclic carbonate. However, no peak at ~1749 cm^{-1} was detected, attributed to the carbonyl group in polycarbonate [14]. The yields of epoxides to corresponding cyclic carbonates were determined by GC (Agilent 7820A) and ethylene glycol dibutyl ether was used as the internal standard.

3. Results and discussion

3.1. *Synthesis of compounds*

Cobaloxime (**1**), organocobaloxime (**2**), and their multinuclear cobaloxime complexes obtained by replacing the intramolecular hydrogen (O–H···O) bridges with Cu(II) complexes of bidentate ligands, 2,2′-bipyridine (bpy), 1,10-phenanthroline (phen),

1,10-phenanthroline-5,6-dione (dione), and 4,4′-ditertbutyl-2,2′-bipyridine (dtbpy) (**3**–**10**) (scheme 1) were investigated for direct synthesis of cyclic carbonates from carbon dioxide and epoxides. The cobaloxime [$ClCo^{III}(LH)_2$(4-*t*-BuPy)] (**1**) was synthesized using well-known synthetic procedures by direct template condensation of three molecules of the corresponding asymmetric dioxime ligands with neutral base on a Co(II) cation as a matrix (scheme 1). **1** was obtained in high yields (86%) using ethanol as solvent. After **1** in ethanol was treated with excess NaOH and $NaBH_4$ dissolved in water, nitrogen was bubbled through the resulting solution for 30 min and the mixture was

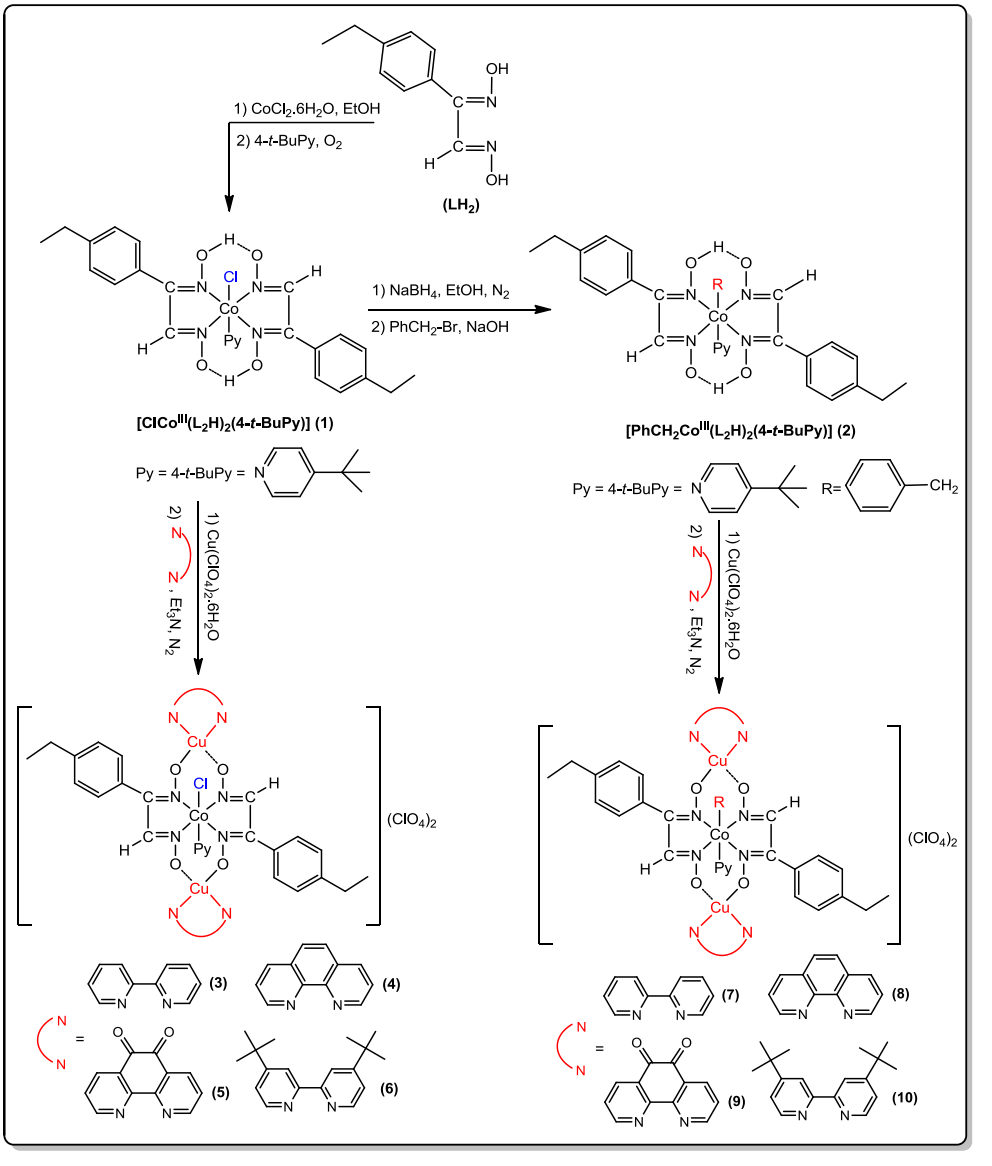

Scheme 1. The structure of the proposed cobaloxime and organocobaloxime complexes (**1**–**10**).

cooled to 2 °C with stirring. Then, an excess of benzyl bromide was added by syringe and the solution turned to gold yellow. The chloride in **1** was replaced by the benzyl to form organocobaloxime [$PhCl_2Co^{III}(LH)_2$(4-*t*-BuPy)] (**2**) with yields of over 76% (scheme 1). The intramolecular hydrogen (O–H···O) bridges were replaced by Cu(II) complexes to form multinuclear **3**–**10** by stirring a 1 : 2 ratio of **1** or **2** and the corresponding $Cu(ClO_4)_2 \cdot 6H_2O$ and linked ligands in ethanol solution. The multinuclear complexes were isolated in yields of 68–74% (scheme 1). We have attempted to prepare single crystals of all compounds (**1**–**10**) in different solvents and techniques, but we could not prepare suitable single crystals. However, the spectroscopic results, ^1H and ^{13}C NMR for diamagnetic **1** and **2**, FT-IR, UV–vis, elemental analysis, melting point measurements, LC-MS spectroscopy, molar conductivity measurements, magnetic susceptibility techniques, and cyclic voltammetry (CV) showed a high probability that these compounds are the proposed structures. **CAUTION (!):** Although no problems were encountered in the present study, perchlorate salts are potentially explosive and should be handled only in small quantities.

3.2. *Structure and characterization*

Infrared spectra of **1** and **2** and trinuclear **3**–**10** are compared with those of the free unsymmetric dioxime to determine the coordination sites that may be involved in chelation. There are some guide peaks in the infrared spectra of the different cobaloximes, which help achieve this goal. The FT-IR results of the unsymmetric dioxime are given in our earlier paper [6]. Thus, in this study, in order to study the binding properties of the mononuclear cobaloxime (**1**), organocobaloxime (**2**), and trinuclear cobaloxime and organocobaloxime complexes (**3**–**10**), FT-IR spectra of **1** and **2** are compared to **3**–**10**. FT-IR spectra of **1** and **2** showed a weak deformation band at 1718 and 1724 cm^{-1}, indicative of intramolecular hydrogen-bonded bending vibrations (O–H···O) associated with N_4-type donor quadridentate Co(III) dioxime complexes. In FT-IR spectra of **3**–**10**, the intramolecular hydrogen bond was not observed because the H-bond of cobaloxime (**1**) and organocobaloxime (**2**) was replaced by $Cu_2(bpy)_2$, $Cu_2(phen)_2$, $Cu_2(dione)_2$, or $Cu_2(dtbpy)_2$, respectively [19]. The strong peaks at 1618 and 1609 cm^{-1} for **1** and **2** can be attributed to υ(C=N) [20]. For **3**–**10**, this peak is at 1606–1602 cm^{-1}. A shift to lower frequency for the vibration corresponding to C=N favors formation of coordination bonds between Co(III) and azomethine. In the FT-IR spectra of **5** and **9**, a new strong band is observed at 1722 cm^{-1} for **5** and at 1722 and 1710 cm^{-1} for **9**, assigned to υ(C=O). In **3**–**10**, perchlorate show strong antisymmetric stretching bands at 1090 cm^{-1} and sharp antisymmetric stretching bands at 625–623 cm^{-1}, an indication of uncoordinated perchlorate anions [21, 22]. These values are in agreement with those for cobaloxime (**1**), organocobaloxime (**2**), and the trinuclear cobaloxime and organocobaloxime (**3**–**10**) complexes. FT-IR vibrations are given in the experimental section for all compounds.

The UV–visible spectral results for **1**–**10** were measured in C_2H_5OH and CH_2Cl_2 solutions from 200 to 1100 nm. Cobaloxime compounds show three characteristic absorptions, attributed to $\pi \rightarrow \pi^*$ or $n \rightarrow \pi^*$ transitions of the dioxime or bidentate ligands. The more intense bands at 224–335 nm in C_2H_5OH and 223–326 nm in CH_2Cl_2 are assumed to be predominantly intraligand, but their energies depend on the nature of the complexed metal. The difference in energy of the UV absorptions when comparing **1** and **2** with **3**–**10** indicates a metal orbital contribution to the transition, while the bidentate ligands

(bpy, phen, dione, and dtbpy) exert only a minimal influence [23]. The moderately intense absorptions at 367–414 (in C_2H_5OH) and 376–416 (in Cl_2CH_2) nm are almost identical and are attributable to dioxime-to-Co(III) or bidentate ligand to Cu(II) CT transitions. The other characteristic absorptions were *d–d* transitions in the visible region, but we did not observe these bands for all compounds, most probably due to their very low intensities. Complexes **3**, **4**, and **6** at high concentrations displayed Laporte forbidden *d–d* transitions at 619–642 nm from Cu(II).

^{1}H and ^{13}C NMR data for **1** and **2** in DMSO-d_6 are reported in the experimental section. Since **3**–**10** are paramagnetic, their NMR spectra could not be obtained. One major difference in **1** and **2** was the presence of a benzyl group instead of a chloride as axial ligand in **2**. The change of **1**–**2** was confirmed by changes observed in the aromatic region of the ^{1}H NMR spectra and by the appearance of a characteristic singlet at 5.46 ppm attributed to the Ph–C$\underline{H}_2$ of the benzyl group as axial ligand. Chemical shifts were observed as singlet (11.86 ppm, 2H or 11.69 and 11.47 ppm, 2H) for the *cis/trans*-isomer and the deuterium exchangeable protons of the C=N–O$\underline{H}$ groups of dioxime in ^{1}H NMR spectra of the unsymmetric dioxime ligand described previously [6]. The signal disappeared in the ^{1}H NMR spectrum of **1** and **2**, while new signals appeared and were identified as singlet signals at 18.80 and 18.55 ppm in the former and as singlet at 18.36 and 18.16 ppm in the latter, indicating that the C=N–O$\underline{H}$ was transformed to intramolecular deuterium exchangeable H-bridge (O–$\underline{H}$···O). The presence of a singlet at 11.87 ppm for **1** was attributed to azomethine protons (CH=N). The CH=N NMR of **2** was observed at 8.90 ppm, shifted downfield upon coordination to the metal. This observation also confirmed participation of the iminic nitrogens in coordination. The chemical shift values of the aromatic protons and other protons for **1** and **2** are identical. In the ^{13}C NMR spectrum, carbon resonances of the dioxime ($\underline{C}$=N–OH) are observed at 151.26 and 149.94 ppm for **1** and at 152.45 and 148.96 ppm for **2**. The carbons of aromatic groups were observed at 147.68, 146.16, 145.02, 141.28, 132.07, 130.35, and 128.47 ppm for **1** and 148.03, 146.23, 145.08, 140.86, 137.01, 132.15, 130.28, 129.64, 128.46, and 128.39 and Ph–$\underline{C}H_2$ carbon at 78.43 ppm for **2**. These values are in agreement with those for **1** and **2**. The other NMR chemical data are given in the experimental section for **1** and **2**.

The LC-MS spectra of **1**–**10** were taken as evidence for the formation of the proposed structures (figures 1–3). The peak positions and the isotopic distributions have been well assigned, and the results are listed in the experimental section. The LC-MS spectra of all compounds show the molecular ion peak at m/z = 612.3 amu [M^+] confirming the proposed formula for **1** (see figure 1), at m/z = 667.7 amu [M^+] confirming the proposed formula for **2** (see figure 2), at m/z = 1248.4 amu [M^+] confirming the proposed formula for **3**, at m/z = 1296.5 amu [M^+] confirming the proposed formula for **4**, at m/z = 1357.2 amu [$(M+H)^+$] confirming the proposed formula for **5** (see figure 3), at m/z = 1472.3 amu [M^+] confirming the proposed formula for **6**, at m/z = 1304.2 amu [M^+] confirming the proposed formula for **7**, at m/z = 1352.3 amu [M^+] confirming the proposed formula for **8**, at m/z = 1412.2 amu [M^+] confirming the proposed formula for **9**, and at m/z = 1529.4 amu [$(M+H)^+$] confirming the proposed formula for **10**. The molecular ion peak is in good agreement with the suggested molecular formula verified by elemental analyses [24].

All the compounds are practically insoluble in water, but are sufficiently soluble in DMF and other organic solvents such as CH_2Cl_2, C_2H_5OH, and DMSO. For consistency, solution studies were carried out in DMF solution [25]. The molar conductivity values of 10^{-3} M solution in DMF are 16–17 Ω^{-1} cm^2 M^{-1} for **1** and **2**, indicating a non-electrolyte.

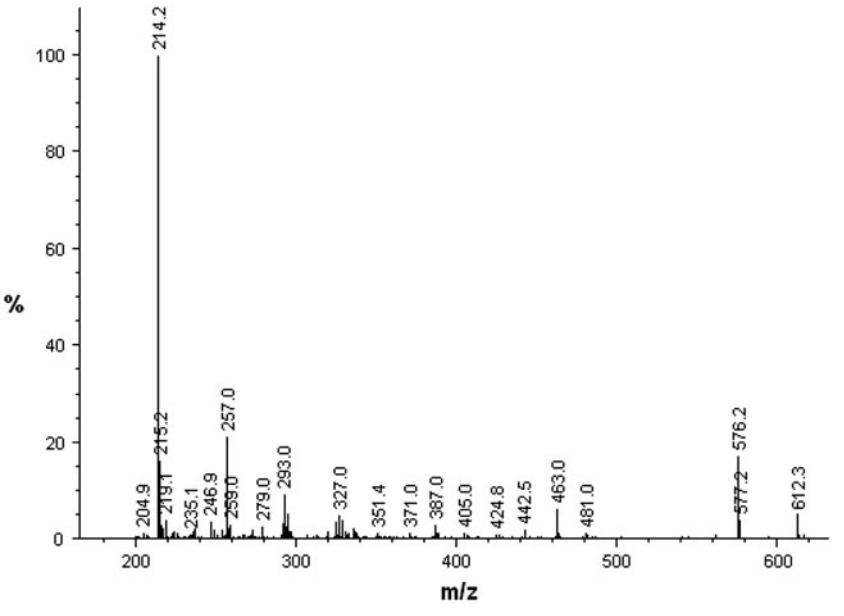

Figure 1. The LC-MS spectra of **1**.

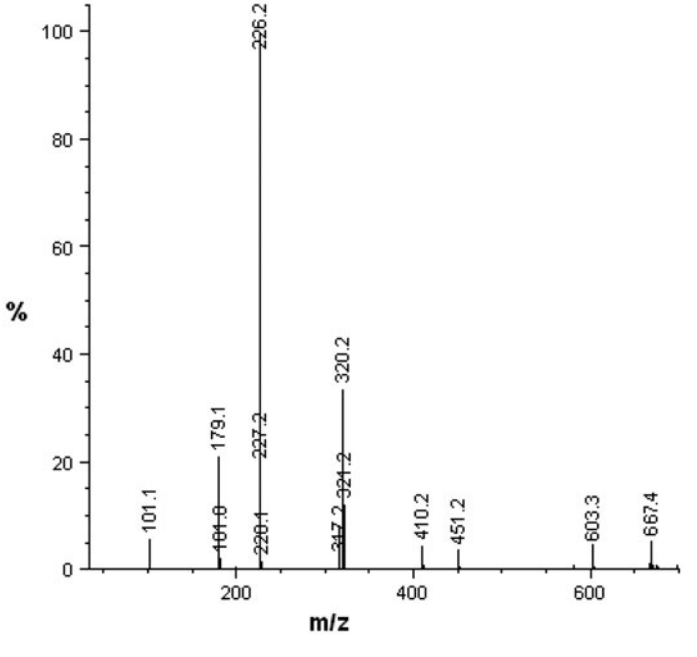

Figure 2. The LC-MS spectra of **2**.

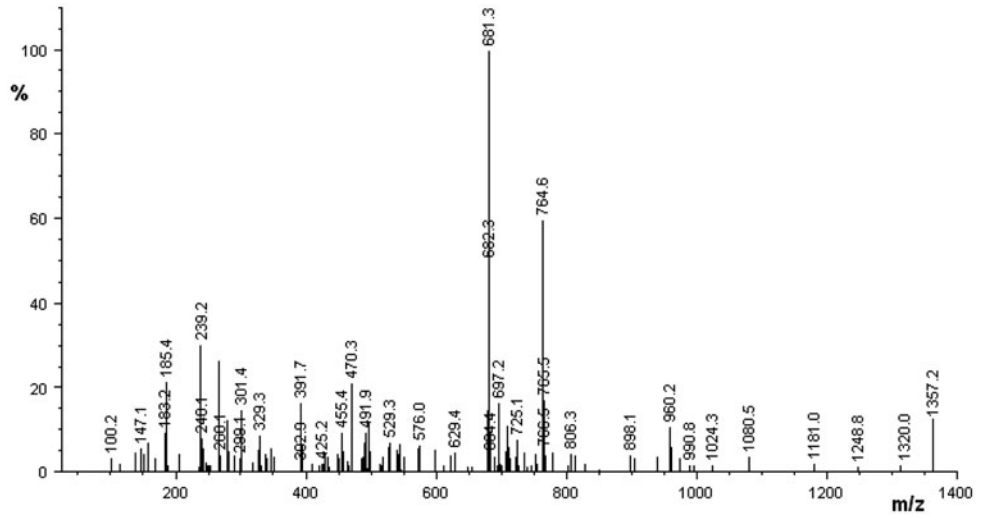

Figure 3. The LC-MS spectra of **5**.

Complexes **3**–**10** had molar conductance values of 158–146 Ω^{-1} cm^2 M^{-1}, suggesting 1 : 2 electrolytes [26], consistent with the presence of 2 ClO_4^- counterions.

Magnetic susceptibility measurements provide further data to characterize the structure of the cobaloxime, organocobaloxime, and other complexes. Magnetic moments measurements of all mono and trinuclear complexes were carried out at 25 °C after necessary diamagnetic corrections using Pascal's table. **1** and **2** are diamagnetic, indicating low-spin (**S** = 0) square-planar d^8-systems and confirming that the cobalt center is +3. The trinuclear cobaloxime complexes (**3**–**10**) are paramagnetic at 1.64–1.55 B.M., comparable to the expected spin-only value (1.73 μB) for one unpaired electron and confirming the formal +2 oxidation state of copper. Complexes **3**–**10** possess antiferromagnetic properties at room temperature by strong intramolecular antiferromagnetic spin exchange interaction as reported previously for the intramolecular metal complexes with dioximate bridges [27].

3.3. *Electrochemical properties*

The electrochemical behaviors of **1**–**10** were studied by CV techniques in DMSO containing 0.2 M TBAP where an Ag/AgCl electrode was used as a reference electrode. The related data obtained in this work are tabulated in table 1. Two examples of the cyclic voltammograms of **2** and **4** are given in figures 4 and 5. As seen from figure 4, **2** has two cathodic peaks in the Ag/AgCl electrode system without corresponding anodic peaks which indicates irreversible redox processes. The cathodic peak potentials of the reduction processes were observed at E_{pc} = −1.363 and −1.775 V. These reduction processes are based on the oxime ligand (L/L^{2-}) and central metal atom (Co^{3+}/Co^{2+}). The ligand-based reduction process of **2** was negatively shifted compared to that of the nickel oxime complex previously studied [6] as a result of replacing Ni^{2+} with Co^{3+} in the complex structure. Although **2** displayed a Co^{3+}/Co^{2+} reduction process, **1** had no metal-based redox process. The multinuclear cobaloxime (**4**) exhibited three reduction and one oxidation processes

Table 1. Voltammetric data for **1** and **2**, and their multinuclear cobaloxime complexes containing Cu^{2+} ions (**3**–**10**) in DMSO-TBAP.

Metal complexes	L/L^{-2} E_{pc} (V)	Co^{3+}/Co^{2+} E_{pc} (V)	Cu^{2+}/Cu^{+} E_{pc} (V)	Cu^{2+}/Cu^{3+} E_{pa} (V)
1	−1.312	–	–	–
2	−1.363	−1.775	–	–
3	−1.415	–	0.056	–
4	−1.474	−1.545	0.005	0.800
5	−1.501	–	0.617	0.014
6	−1.522	–	0.131	–
7	−1.387	–	0.033	–
8	−1.512	–	0.016	–
9	−1.371	–	–	–
10	−1.387	–	–	–

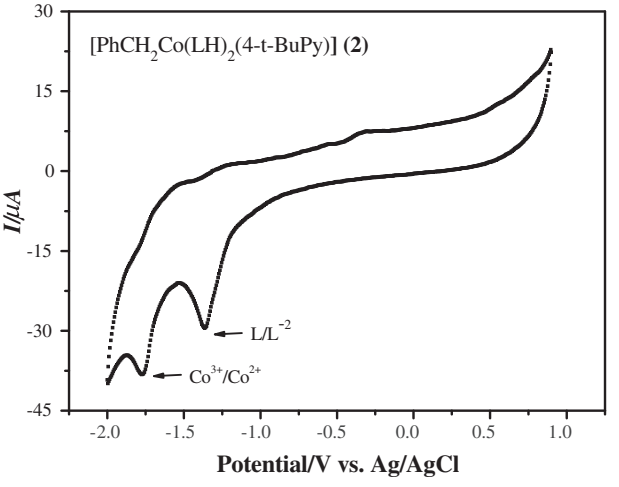

Figure 4. The cyclic voltammogram of **2** on GC electrode in DMSO/0.2 M TBAP at 0.1 V s^{-1} scan rate.

which were attributed to the oxime ligand (L/L^{2-}) and metal ions (Co^{3+}/Co^{2+}, Cu^{2+}/Cu^{+} and Cu^{2+}/Cu^{3+} processes) (figure 5 and table 1). All redox processes have irreversible reduction–oxidation processes because of the high value for the anodic-to-cathodic peak separation and the smaller anodic-to-cathodic peak current ratio. This result was similar to that observed for the multinuclear nickel oxime previously studied [6] except for the Co^{3+}/Co^{2+} reduction process. Observable shifts in the redox potentials and lack of some reduction or oxidation processes for **3**–**10** are due to changes in the nature of ligands coordinated by copper.

3.4. *Catalytic properties*

Cycloaddition of carbon dioxide with epoxide in the presence of 0.1% cobaloxime complexes (**1–10**) was conducted as a model reaction (scheme 1) and the results are compiled in table 2. The catalytic experiments were carried out under optimized conditions, which

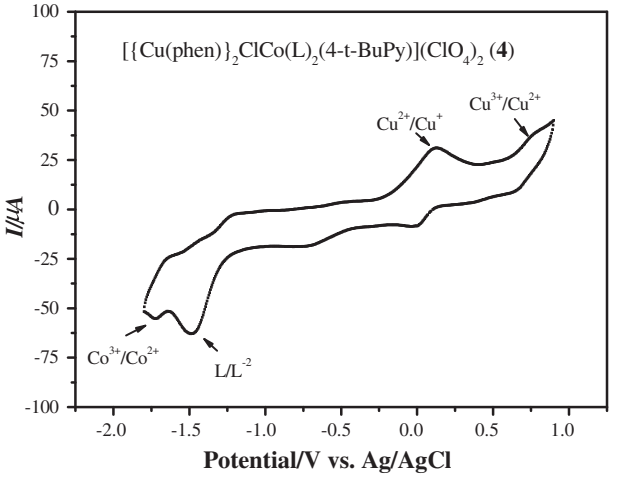

Figure 5. The cyclic voltammogram of **4** on GC electrode in DMSO/0.2 M TBAP at 0.1 V s^{-1} scan rate.

were determined in previous studies [28–30]. The cobaloxime complexes (**1**–**10**), when 4-dimethylamino pyridine (DMAP) was used as co-catalysts, showed catalytic activity and selectivity for the conversion of CO_2 into cyclic carbonates using epoxide derivatives as substrate and solvent.

3.4.1. CO_2 coupling reaction with ECH in the presence of various catalysts. The cobaloxime (**1**) and DMAP showed high catalytic activity with 75.9% yield and 98.6%

Table 2. Synthesis of epichlorohydrin carbonate from epichlorohydrin and CO_2 via synthesized cobaloxime complexes as catalysts.

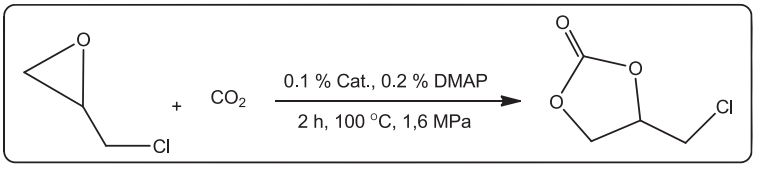

Cat.	Yield[a] (%)	Selectivity[a] (%)	TON[b]	TOF[c] (h^{-1})
1	75.9	98.6	759	380
2	69.3	98.5	693	347
3	14.9	95.2	149	75
4	3.2	82.8	320	160
5	27.6	96.7	276	138
6	20.6	96.7	206	103
7	48.2	97.6	482	241
8	4.3	83.4	430	215
9	3.1	72.7	310	155
10	5.1	90.1	510	255

[a]Yield and selectivity of epichlorohydrin to corresponding epichlorohydrin carbonate were determined by GC.
[b]Moles of cyclic carbonate produced per mole of catalyst.
[c]The rate is expressed in terms of the turnover frequency {TOF [mol of product (mol of catalyst h)$^{-1}$] = turnovers/h}.

selectivity for the coupling of CO_2 and epichlorohydrin (figure 6). Cobaloxime **1** showed best catalytic performance (figure 6) with epichlorohydrin as substrate. The two precursor complexes (**1** and **2**) showed better activity than their analogs (**3**–**10**). The lower catalytic efficiencies of eight metalic complexes (**3**–**10**) may be due to the low solubility of them in the epoxide (epichlorohydrin).

3.4.2. CO_2 coupling reaction with other epoxides in the presence of 1 as catalyst. Using **1** as the most active catalyst (figure 6), we have carried out some catalytic reactions changing the temperature, time, solvent, pressure, and epoxide to find the best reaction conditions. In addition to epichlorohydrin (ECH), 1,2-epoxybutane (EB), propylene oxide (PO), styrene oxide (SO), and cyclohexene oxide (CHO) were tested as substrates. **1** was not effective for the epoxides (EB, PO, SO, and CHO) (figure 7). Whereas, using the ECH as epoxide, good activity and selectivity were achieved at the same catalytic conditions. This result may be because the styrene oxide (SO) and 1,2-epoxybutane (EB) are bulkier epoxides compared to epichlorohydrin (ECH), and at the same time, the low

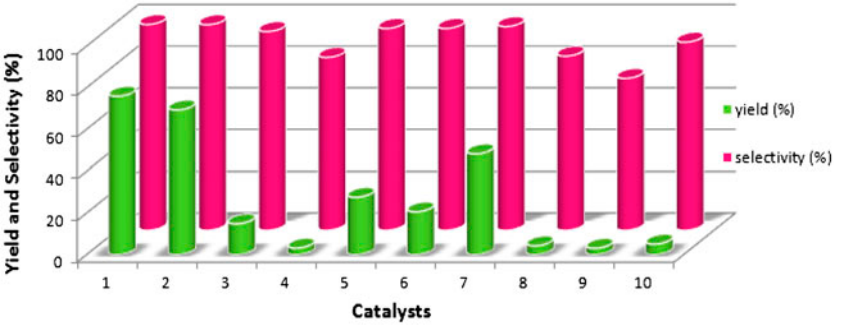

Figure 6. The comparison of catalysts for the formation of epichlorohydrin to corresponding cyclic carbonate (4-(chloromethyl)-1,3-dioxolan-2-one) at the same catalytic conditions.

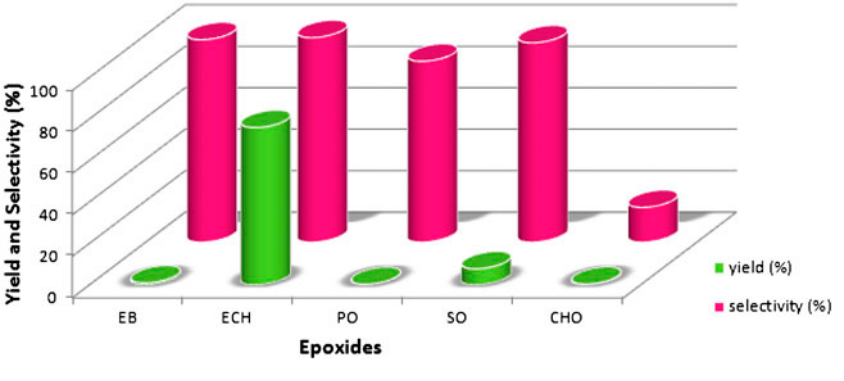

Figure 7. The conversion of epoxides to corresponding cyclic carbonates at the same catalytic conditions with **1** as catalyst.

reactivity of the β-carbon atom of styrene oxide (SO) and 1,2-epoxybutane (EB) could be responsible. However, the Co centers may be involved in binding to the olefin unit of styrene oxide (SO), but for 1,2-epoxybutane (EB) this cannot be the case. In addition to the above statements, many parameters such as biphasic reaction media, polarity differences between catalyst, substrates, and CO_2 could play a role. The results of optimization conditions such as reaction temperature, epoxide, time, and CO_2 pressure were very similar with both homogeneous and heterogeneous systems that were previously reported [30–32].

3.4.3. Influence of solvents on the ECHC (4-(chloromethyl)-1,3-dioxolan-2-one) synthesis. In addition to MeOH, toluene, dichloromethane, EtOH, $CHCl_3$, isopropyl alcohol, DMF, and DMSO were tested as solvents. It is clear that the solvent is not necessary according to the catalytic test results (figure 8). This is important in green chemistry.

3.4.4. Influence of reaction temperature on the ECHC (4-(chloromethyl)-1,3-dioxolan-2-one) synthesis. It was found that the yield of ECHC (epichlorohydrin carbonate) was strongly affected by reaction temperature. ECH reached 96.6% yield and 98.7% selectivity within 2 h, with CO_2 pressure 1.6 MPa at 125 °C (figure 9). As shown in figure 9, the yield and selectivity of ECHC increased with the reaction temperature to 125 °C, whereas a further increase in temperature caused a decrease in the selectivity and catalytic activity, possibly due to more side products formed at higher temperature (such as 3-chloropropane-1,2-diol). Apparently, 125 °C could be the optimal temperature for the reaction (figure 9).

3.4.5. Effect of reaction pressure on the ECHC (4-(chloromethyl)-1,3-dioxolan-2-one) synthesis. Figure 10 shows the effect of CO_2 pressure on the yield of ECHC using **1** as catalyst. The selectivity is independent of the CO_2 pressure range from 0.5 to 4 MPa and ECHC yield shows no significant change with variation of CO_2 pressure. However, increasing CO_2 pressure above 1.6 MPa decreased the yield and turnover frequency (TOF) (figure 10). A similar effect was reported previously by us [31]. As easily seen, the best ECHC yield could be achieved at 1.6 MPa.

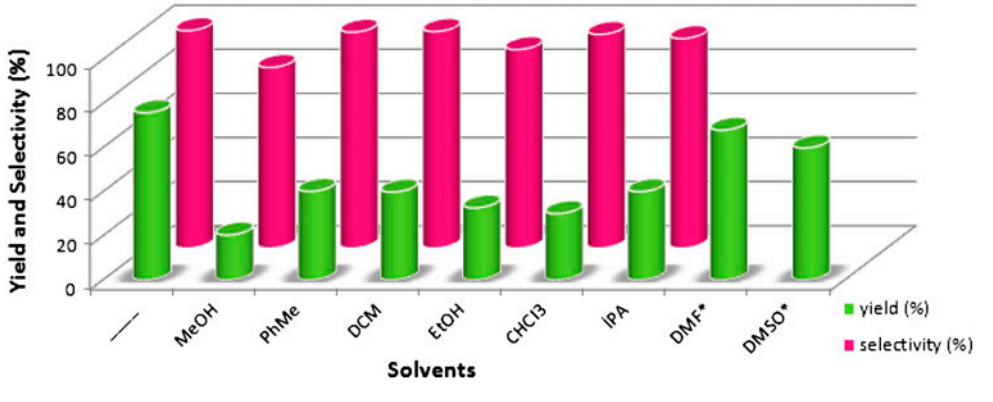

Figure 8. Conversion and selectivity of epichlorohydrin from changing solvent with **1** as catalyst.
*DMF (dimethylformamide) and DMSO (dimethylsulfoxide) were used as a solvent which has the same retention time with diol (as a byproduct). So, the selectivity could not be calculated.

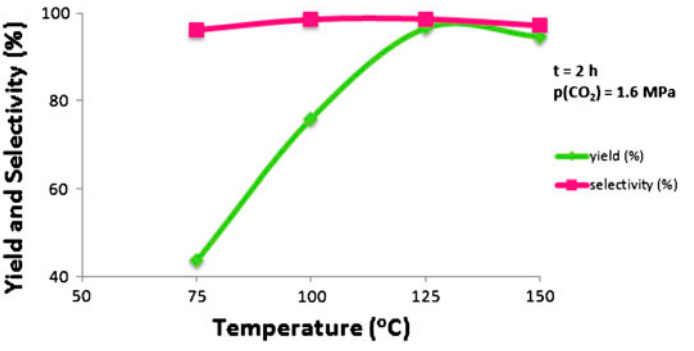

Figure 9. Conversion and selectivity of epichlorohydrin as a function of temperature with **1** as catalyst.

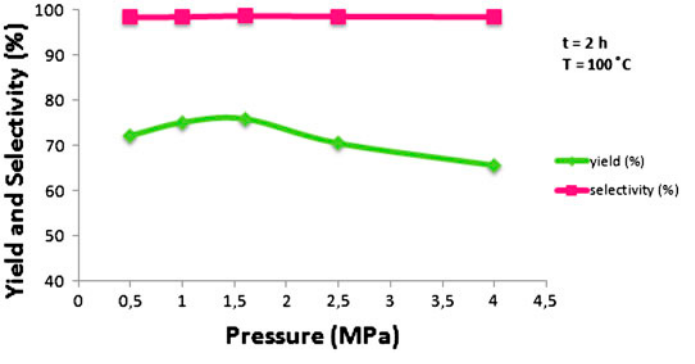

Figure 10. Conversion and selectivity of epichlorohydrin as a function of pressure with **1** as catalyst.

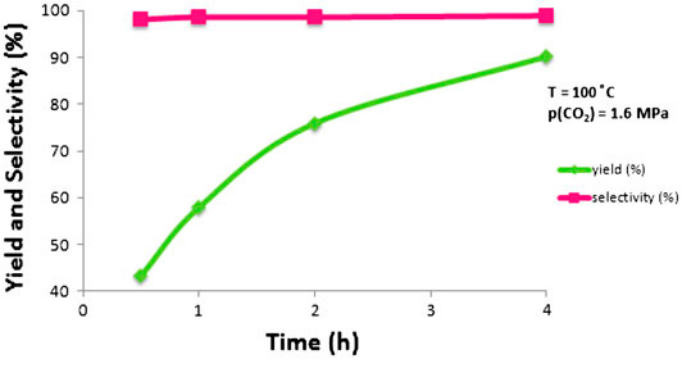

Figure 11. Conversion and selectivity of epichlorohydrin as a function of time with **1** as catalyst.

3.4.6. Reaction time dependence on ECHC (4-(chloromethyl)-1,3-dioxolan-2-one) yield. The influence of reaction time on the ECHC synthesis using **1** is given in figure 11. The reactions were performed in the presence of 4.5×10^{-5} M of **1** at 100 °C under 1.6 MPa pressure. The results indicate that the ECH reached 90.2% yield within 4 h, with CO_2 pressure 1.6 MPa at 100 °C (figure 11).

4. Conclusion

The new cobaloxime (**1**), organocobaloxime (**2**), and their intramolecular hydrogen (O–H···O) bridges replaced by Cu(II) complexes giving multinuclear cobaloximes (**3**–**10**) were synthesized and characterized by elemental analysis, ^{1}H and ^{13}C NMR spectra, FT-IR spectra, UV–vis spectra, LC-MS spectra, molar conductivity measurements, melting point measurements, and magnetic susceptibility measurements. Their electrochemical properties were investigated using CV techniques in DMSO solution. All redox processes have irreversible reduction–oxidation processes because of the high value for the anodic-to-cathodic peak separation and the smaller anodic-to-cathodic peak current ratio. There are many literature reports that the cobaloxime, dicobaloxime, and the intramolecular hydrogen (O–H···O) bridges replaced by Cu(II) ions or other metal ions containing complexes have been used as catalysts in coupling reactions of carbon dioxide (CO_2) and different epoxides. Solvent is not necessary to be used according to the catalytic test results. This is an important phenomenon in green chemistry. Amazingly, the most active catalyst **1** was not effective in the epoxides (EB, PO, SO, and CHO). Using epichlorohydrin as epoxide, good activity and selectivity were achieved under the same catalytic conditions. This result may be because the styrene oxide (SO) and 1,2-epoxybutane (EB) are bulkier epoxides compared to epichlorohydrin (ECH), and at the same time, the low reactivity of β-carbon atom of styrene oxide (SO) and 1,2-epoxybutane (EB) could be responsible. However, the Co centers may be involved in binding to the olefin of styrene oxide (SO), but for 1,2-epoxybutane (EB), this cannot be the case. Parameters such as biphasic reaction media, polarity differences between catalyst, substrates, and CO_2 could play a role.

Acknowledgment

This work was supported by the Technological and Scientific Research Council of Turkey TUBITAK (TBAG Project Nos: 111T944 and 110T655).

References

[1] M. Bhuyan, M. Laskar, D. Mandal, B.D. Gupta. *Organometallics*, **26**, 3559 (2007).
[2] J. Niklas, K.L. Mardis, R.R. Rakhimov, K.L. Mulfort, D.M. Tiede, O.G. Poluektov. *J. Phys. Chem. B*, **116**, 2943 (2012).
[3] A. Fihri, V. Artero, M. Razavet, C. Baffert, W. Leibl, M. Fontecave. *Angew. Chem. Int. Ed.*, **47**, 564 (2008).
[4] G.N. Schrauzer, J.W. Sibert, R.J. Windgassen. *J. Am. Chem. Soc.*, **90**, 6681 (1968).
[5] B. Krautler, D. Arigoni, B.T. Golding. *Vitamin B12 and B12-Proteins*, Wiley-VCH, Weinheim (1998).
[6] A. Kilic, A.A. Palali, M. Durgun, Z. Tasci, M. Ulusoy, M. Dagdevren, I. Yilmaz. *Inorg. Chim. Acta*, **394**, 635 (2013).
[7] S. Kumar, S.L. Jain, B. Sain. *Catal. Today*, **198**, 204 (2012) and references cited therein.

[8] M. Aresta, A. Dibenedetto, I. Tommasi. *Energ. Fuels*, **15**, 269 (2001).
[9] C.J. Liu, R. Mallinson, M. Aresta (Eds.). *Preface, ACS Symposium Series (e-book) Utilization of Green House Gases*, Vol. 852, pp. ix–xi (2003).
[10] C.J. Whiteoak, N. Kielland, V. Laserna, E.C.E. Adan, E. Martin, A.W. Kleij. *J. Am. Chem. Soc.*, **135**, 1228 (2013) and references cited therein.
[11] K. Huang, C.L. Sun, Z.J. Shi. *Chem. Soc. Rev.*, **40**, 2435 (2011).
[12] D.J. Darensbourg, R.M. Mackiewicz, A.L. Phelps, D.R. Billodeaux. *Acc. Chem. Res.*, **37**, 836 (2004).
[13] K.C. Nicolaou, Z. Yang, J.J. Liu, H. Ueno, P.G. Nantermet, R.K. Guy, C.F. Claiborne, J. Renaud, E.A. Couladouros, K. Paulvannanand, E.J. Sorensen. *Nature*, **367**, 630 (1994).
[14] D. Bai, G. Nian, G. Wang, Z. Wang. *Appl. Organomet. Chem.*, **27**, 184 (2013).
[15] D.R. Moore, M. Cheng, E.B. Lobkovsky, G.W. Coates. *Angew. Chem. Int. Ed.*, **41**, 2599 (2002).
[16] T. Takata, J.C. Chio, H. Yasuda. *Chem. Rev.*, **107**, 2365 (2007).
[17] A. Earnshaw. *Introduction to Magnetochemistry*, p. 4, Academic Press, London (1968).
[18] M. Yamada, Y. Tanaka, Y. Yoshimoto, S. Kuroda, I. Shimao. *Bull. Chem. Soc. Jpn.*, **65**, 1006 (1992).
[19] A. Kilic, F. Durap, M. Aydemir, A. Baysal, E. Tas. *J. Organomet. Chem.*, **693**, 2835 (2008).
[20] A. Yılmaz, B. Taner, P. Deveci, A.Y. Obalı, U. Arslan, E. Sahin, H.I. Ucan, E. Ozcan. *Polyhedron*, **29**, 2991 (2010).
[21] M.R. Rosenthal. *J. Chem. Educ.*, **50**, 331 (1973).
[22] A. Kilic, F. Durap, A. Baysal, M. Durgun. *J. Inclusion Phenom. Macrocyclic Chem.*, **67**, 423 (2010).
[23] A.M. Whyte, B. Roach, D.K. Henderson, P.A. Tasker, M.M. Matsushita, K. Awaga, F.J. White, P. Richardson, N. Robertson. *Inorg. Chem.*, **50**, 12867 (2011).
[24] S.C. Ruchi. *Spectrochim. Acta, Part A*, **103**, 338 (2013).
[25] S. Sarkar, S. Majumder, S. Sasmal, L. Carrella, E. Rentschler, S. Mohanta. *Polyhedron*, **50**, 270 (2013).
[26] K. Karaoglu, T. Baran, I. Degirmencioglu, K. Serbest. *Spectrochim. Acta, Part A*, **79**, 867 (2011).
[27] S. Karabocek, N. Karabocek. *Polyhedron*, **16**, 1771 (1997).
[28] A. Kilic, M. Durgun, M. Ulusoy, E. Tas. *J. Chem. Res.*, **11**, 622 (2011).
[29] M. Ulusoy, A. Kilic, M. Durgun, Z. Tasci, B. Cetinkaya. *J. Organomet. Chem.*, **696**, 1372 (2011).
[30] A. Kilic, M. Ulusoy, M. Durgun, Z. Tasci, I. Yilmaz, B. Cetinkaya, E. Tas. *Appl. Organomet. Chem.*, **24**, 446 (2010).
[31] M. Ulusoy, E. Cetinkaya, B. Cetinkaya. *Appl. Organomet. Chem.*, **23**, 68 (2009).
[32] Z. Tasci, M. Ulusoy. *J. Organomet. Chem.*, **713**, 104 (2012).